


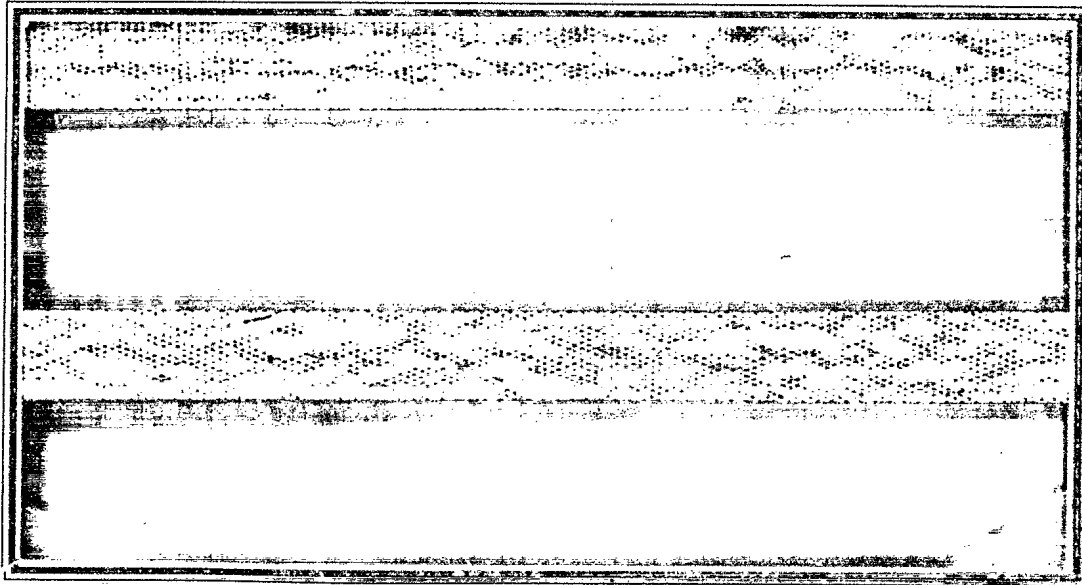
CLASSIFICATION	SYSTEM NUMBER	499218
UNCLASSIFIED		
TITLE		
COMPUTATIONAL FLUID DYNAMIC ANALYSIS OF THE CAN-1 HYPERSONIC RESEARCH PROJECTILE		
System Number:		
Patron Number:		
Requester:		
Notes:		
DSIS Use only:		
Deliver to:		

Report Documentation Page			Form Approved OMB No. 0704-0188		
Public reporting burden for the collection of information is estimated to average 1 hour per response, including the time for reviewing instructions, searching existing data sources, gathering and maintaining the data needed, and completing and reviewing the collection of information. Send comments regarding this burden estimate or any other aspect of this collection of information, including suggestions for reducing this burden, to Washington Headquarters Services, Directorate for Information Operations and Reports, 1215 Jefferson Davis Highway, Suite 1204, Arlington VA 22202-4302. Respondents should be aware that notwithstanding any other provision of law, no person shall be subject to a penalty for failing to comply with a collection of information if it does not display a currently valid OMB control number.					
1. REPORT DATE JUN 1996		2. REPORT TYPE		3. DATES COVERED	
4. TITLE AND SUBTITLE Computational Fluid Dynamic Analysis of the CAN-1 Hypersonic Research Projectile		5a. CONTRACT NUMBER			
		5b. GRANT NUMBER			
		5c. PROGRAM ELEMENT NUMBER			
6. AUTHOR(S)		5d. PROJECT NUMBER			
		5e. TASK NUMBER			
		5f. WORK UNIT NUMBER			
7. PERFORMING ORGANIZATION NAME(S) AND ADDRESS(ES) Defence R&D Canada - Valcartier, 2459 Pie-XI Blvd North, Quebec (Quebec) G3J 1X5 Canada, ,		8. PERFORMING ORGANIZATION REPORT NUMBER			
9. SPONSORING/MONITORING AGENCY NAME(S) AND ADDRESS(ES)		10. SPONSOR/MONITOR'S ACRONYM(S)			
		11. SPONSOR/MONITOR'S REPORT NUMBER(S)			
12. DISTRIBUTION/AVAILABILITY STATEMENT Approved for public release; distribution unlimited.					
13. SUPPLEMENTARY NOTES					
14. ABSTRACT In an effort to broaden our knowledge base on hypersonic aerodynamics, DREV conducted a Computational Fluid Dynamics (CFD) analysis of a hypersonic projectile, and successfully validated the analysis with results from free flight trials. Quantitative information (aerodynamic coefficients, shock wave interaction position, separation bubble position, etc.) was accurately obtained by the CFD code, as indicated by the good agreement with experimental results. The influence of the shock wave/flame interaction on some of these quantities was also identified. On the qualitative side, the modelling of flow characteristics such as shock patterns and positions, flow separation effects, etc. in a hypersonic environment has been accomplished. In addition, comparisons between these results and those from a numerical analysis from the Defence Research Agency (DRA) have shown that they provide similar values.					
15. SUBJECT TERMS					
16. SECURITY CLASSIFICATION OF:			17. LIMITATION OF ABSTRACT	18. NUMBER OF PAGES 40	19a. NAME OF RESPONSIBLE PERSON
a. REPORT unclassified	b. ABSTRACT unclassified	c. THIS PAGE unclassified			



UNCLASSIFIED

DEFENCE RESEARCH ESTABLISHMENT
CENTRE DE RECHERCHES POUR LA DÉFENSE
VALCARTIER, QUÉBEC



RESEARCH AND DEVELOPMENT BRANCH
DEPARTMENT OF NATIONAL DEFENCE
CANADA
BUREAU - RECHERCHE ET DÉVELOPPEMENT
MINISTÈRE DE LA DÉFENSE NATIONALE

Canada

SANS CLASSIFICATION

UNCLASSIFIED

DEFENCE RESEARCH ESTABLISHMENT
CENTRE DE RECHERCHES POUR LA DÉFENSE
VALCARTIER, QUÉBEC

DREV - TM - 9607

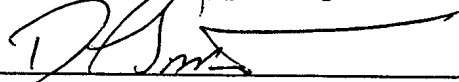
COMPUTATIONAL FLUID DYNAMIC ANALYSIS
OF THE CAN-1 HYPERSONIC RESEARCH PROJECTILE

by

E. Y. Fournier and A. D. Dupuis

June/juin 1996

Approved by / approuvé par



Chief Scientist / Scientifique en chef

17/7/96

Date

SANS CLASSIFICATION

UNCLASSIFIED

i

ABSTRACT

In an effort to broaden our knowledge base on hypersonic aerodynamics, DREV conducted a Computational Fluid Dynamics (CFD) analysis of a hypersonic projectile, and successfully validated the analysis with results from free flight trials. Quantitative information (aerodynamic coefficients, shock wave interaction position, separation bubble position, etc.) was accurately obtained by the CFD code, as indicated by the good agreement with experimental results. The influence of the shock wave/flare interaction on some of these quantities was also identified. On the qualitative side, the modelling of flow characteristics such as shock patterns and positions, flow separation effects, etc. in a hypersonic environment has been accomplished. In addition, comparisons between these results and those from a numerical analysis from the Defence Research Agency (DRA) have shown that they provide similar values.

RÉSUMÉ

Dans le but d'approfondir nos connaissances sur les véhicules se déplaçant dans le régime de vitesse hypersonique, une étude des caractéristiques aérodynamiques d'un de ces projectiles fut réalisée au Centre de recherches pour la défense, Valcartier (CRDV), à l'aide de codes numériques. Les résultats de cette étude se comparent avantageusement avec les résultats expérimentaux provenant du corridor aérobballistique du CRDV. De l'information quantitative (coefficients aérodynamiques, position de l'interaction "onde de choc/projectile", position et dimensions de la bulle de séparation, etc.) fut modélisée avec précision par le code numérique, comme le démontre les comparaisons avec les résultats expérimentaux. L'influence de l'interaction "onde de choc/projectile" sur ces quantités fut aussi identifiée. D'un aspect qualitatif, la modélisation des caractéristiques de l'écoulement comme la position et la forme des ondes de choc, les effets de la séparation de l'écoulement, etc. dans un environnement hypersonique fut accomplie d'une manière assez précise. Des comparaisons entre ces résultats et d'autres provenant d'analyses numériques et expérimentales exécutées à DRA (Defence Research Agency, Angleterre), ont présenté des résultats relativement semblables.

UNCLASSIFIED

iii

TABLE OF CONTENTS

ABSTRACT / RÉSUMÉ..... i

EXECUTIVE SUMMARY..... v

NOMENCLATURE..... vii

1.0 INTRODUCTION..... 1

2.0 PROJECTILE CONFIGURATION..... 2

3.0 AEROBALLISTIC RANGE..... 3

4.0 COMPUTATIONAL FLUID DYNAMIC CODE..... 3

5.0 RESULTS..... 5

 5.1 Aerodynamic Coefficients..... 5

 5.2 Surface Pressure Survey..... 10

6.0 CONCLUSIONS..... 16

7.0 RECOMMENDATIONS..... 17

8.0 ACKNOWLEDGEMENTS..... 17

9.0 REFERENCES..... 18

 FIGURES 1 to 13

 TABLES I to III

UNCLASSIFIED

v

EXECUTIVE SUMMARY

Higher velocity projectiles are needed to defeat advanced armours. New launch technologies are making higher velocities practical. However, these high velocities ($> \text{Mach} = 4.0$ at sea level) are creating severe difficulties for the flight dynamicist. The aerodynamic characteristics and stability parameters of this type of ordnance will have to be known and understood at these extreme speed (Mach 5 - 8). Specifically, experimental aerodynamic information is sparse at velocities above 1800 m/s and there is a need to augment the flight test data base. Moreover, the CFD techniques used to perform some of these analyses need to be validated at these high velocities. Finally, the structural design of these projectiles to withstand the high temperatures generated during flight, which could produce adverse effects on the aerodynamic and flight performance of these vehicles (ablation), will be critical. There is virtually no data on the behaviour of ablating bodies in free flight at the velocities of interest.

In order to better understand these phenomena, the Defence Research Establishment, Valcartier (DREV) and the Defence Research Agency (DRA, Fort Halstead, England) have been involved in a cooperative project to study the flight dynamic, aerodynamic, and aero-thermal properties of a cone-cylinder-flare hypersonic configuration up to Mach 7. The overall research program consists in conducting aeroballistic range testing of several configurations to determine their aerodynamic coefficients and stability derivatives, and to conduct outdoor firings to measure temperature in flight. In an effort to better understand the physical phenomena associated with this type of flow, a numerical (CFD) analysis of this configuration has been performed as well.

This project resulted in a better understanding of the aerodynamic characteristics of hypersonic flight. It also provided valuable information to the Canadian Forces on the potential of this type of projectile as future anti-armour weapons. In turn, this allowed DREV to exchange aerodynamic and aerothermal information about the flight behavior of hypersonic projectiles with other TTCF members.

UNCLASSIFIED

vii

NOMENCLATURE

C_D	drag coefficient
$C_{N\alpha}$	normal force coefficient slope
$C_{M\alpha}$	pitching moment coefficient slope
d	projectile body diameter (m)
M	freestream Mach number
P	pressure (Pa)
Re_L	Reynolds number (based on projectile length)
T	temperature (K)
ρ	density (kg/m^3)

UNCLASSIFIED

1

1.0 INTRODUCTION

The very high velocities (above Mach 6.0 at sea level) that future ammunition will achieve with the advent of novel gun and missile propulsion technologies, and the requirements to defeat modern and future armour, introduces challenging problems for the aeroballistician. The aerodynamic characteristics and stability parameters associated with these types of projectiles will have to be known and understood at these extreme speed regimes (Mach 5 - 8) before being fielded with operational units. In order to better understand these high velocity phenomena, the Defence Research Establishment, Valcartier (DREV) and the Defence Research Agency (DRA, Fort Halstead, England) have been involved in a cooperative research project to study the flight dynamic, aerodynamic, and aero-thermal properties of a cone-cylinder-flare hypersonic configuration up to Mach 7.

In an effort to better understand the physical phenomena associated with this type of flow, a numerical (CFD) analysis of one of these configurations has been performed. Results have been compared to experimental values obtained at DREV, to allow for validation of the CFD code for these specific flow conditions, as cases under these conditions had never been simulated with this code previously. It should be acknowledged that the real gas effects were not considered in the present CFD calculations, even for cases at speeds as high as Mach 8.2. A real cost reduction potential has been identified in using CFD simulations in conjunction with a reduced number of experimental testings to produce a more balanced and complete set of data.

The overall research program consists in conducting aeroballistic range testing of several configurations to determine their aerodynamic coefficients and stability derivatives, and to conduct outdoor firings to measure temperature in flight. The phase of the research programme presented in this memorandum covers only the numerical analysis of the aerodynamic characteristics of one of the configurations designed for experimental testing. Pressure surveys, aerodynamic coefficient calculations and visualization of the flow around the projectile were accomplished for a range of Mach numbers and angles of incidence. Comparisons with experimental results from the aeroballistic range, and with CFD results from DRA, were then performed. In addition, possible flow separation at the cylinder-flare intersection has also been investigated.

UNCLASSIFIED

2

This work was conducted as part of a joint cooperative project between Canada and the UK, under the auspices of TTCP-WTP-2, to study the aerodynamic characteristics and aeroheating aspects of several configurations at hypersonic speeds. It was conducted at Defence Research Establishment Valcartier (DREV) between September 1994 and June 1995, under PSC 31D, Weapons Systems (now Project 2EA19 - Hypersonic Flight).

2.0 PROJECTILE CONFIGURATION

The projectile under investigation, designated CAN-1, is shown in Fig. 1 (Ref. 1).

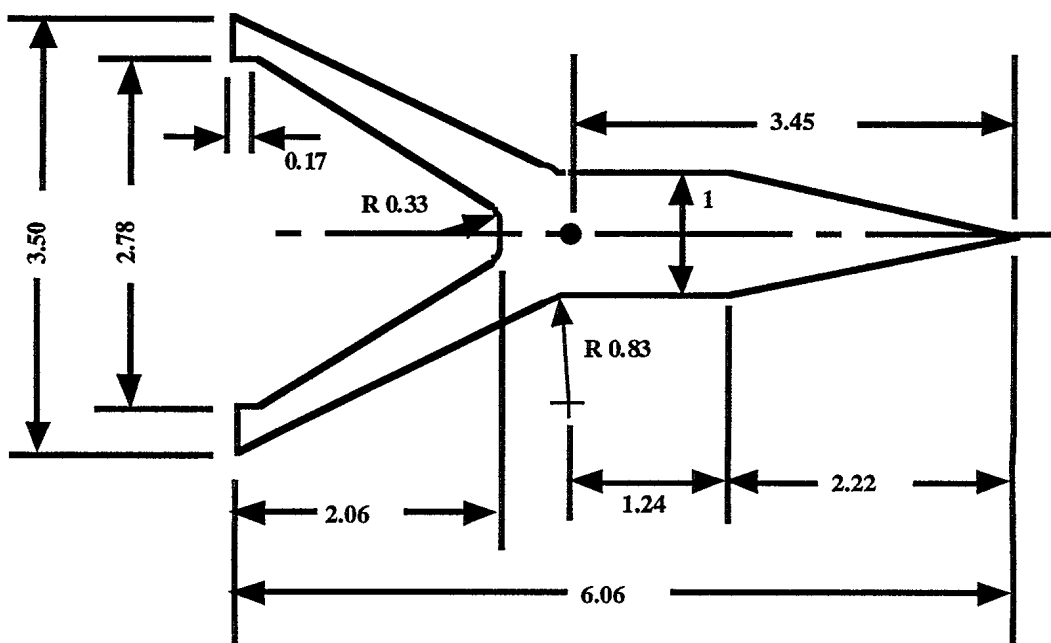


FIGURE 1 - Schematic of the CAN-1 projectile (all dimensions in calibers)

It is a cone-cylinder-flare projectile with a flare angle of 27.6° , designed to obtain a centre of gravity at 3.45 calibers from the nose. The nose is conical with a short cylindrical body section. The large flare angle was selected to study the effects of possible separated flow at the flare/body junction. Additionally, this large flare angle made it possible to study shock wave-boundary layer interactions for large values of Mach number as the shock wave originating at the conical nose of the projectile would intersect with the boundary layer at the surface of the flare. The nominal diameter of this model was 18 mm (diameter of the cylindrical section), which leads to a l/d ratio for this configuration of 6.1.

UNCLASSIFIED

3

3.0 AEROBALLISTIC RANGE

The facility used to accomplish the experimental aspects of the analysis is the DREV aeroballistic range (A/B range). It is used to examine the exterior ballistics of various free-flight configurations, and consists of a gun bay, a control room, and the instrumented range. This range comprises three Schlieren stations followed by 54 orthogonal shadowgraph stations over a range of approximately 260 m (Ref. 2). Ballistic synchro cameras were also employed to provide information on the launch characteristics. The DREV aeroballistic range has a cross sectional area of 6.1m x 6.1m and is temperature and humidity controlled (Fig. 2). Nominal operating conditions are 20°C and 45% relative humidity. For this experiment, flight Reynolds numbers ranged from as high as $Re_L = 1.7 \times 10^7$ at launch, to as low as 5.0×10^6 towards the end of the flight. These Reynolds numbers are sufficiently high that a fully turbulent boundary layer flow had developed along the body. The analysis of the aeroballistic coefficients was carried out at DREV using the Ballistic Range Data Analysis System, BARDAS (Ref. 3). The complete analysis of the test programme can be found in Ref. 4.

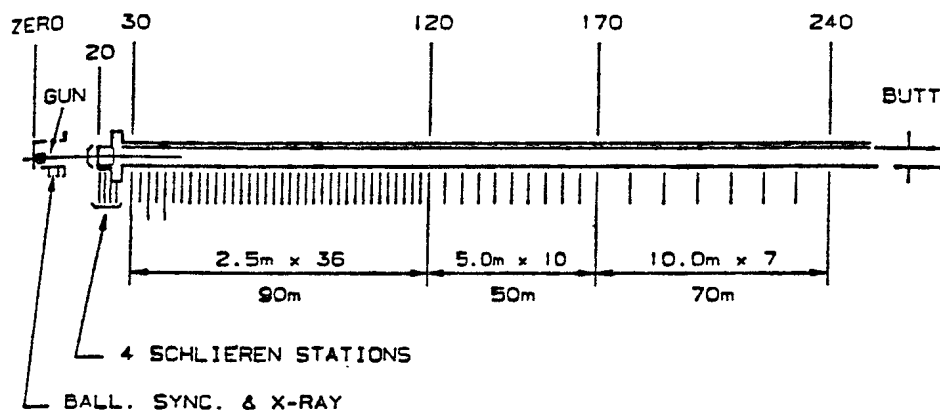


FIGURE 2 - Aeroballistic range photographic station spacing

4.0 COMPUTATIONAL FLUID DYNAMIC CODE

The code used by DREV is the TASCflow¹ Navier-Stokes code developed by Advanced Scientific Computing Ltd (Ref. 5). This code is a fully implicit, finite volume method with a flux element based discretization of geometry that can utilize various

¹ TASCflowTM is a registered Canadian trademark of ASC Ltd.

UNCLASSIFIED

4

numerical upwind schemes to ensure the global conservation of mass, continuity, momentum, and energy. It implements a general non-orthogonal, structured, boundary fitted grid. For this study, a modified linear profile scheme was used, with both laminar and turbulent cases. For the turbulent cases, a standard $k-\epsilon$ turbulence model with wall functions was used to evaluate the Reynolds stresses and thermal diffusion.

The grid generated for this investigation is shown in Fig. 3. It is a three-dimensional grid, due to the requirements of obtaining information on aerodynamic characteristics at angles of attack. Only half of the full geometry of this problem needed to be resolved since this three-dimensional problem is symmetrical. The base flow was not simulated through this mesh. The values of base pressure required in the drag calculations came from semi-empirical sources (Ref. 6). The resulting grid contained 80000 nodes (distribution: $100 \times 32 \times 25$). This grid was assumed sufficient to prevent shock wave reflection off the outer boundary and hence possible downstream flow interference, as well as to ensure full supersonic flow at the outflow boundary.

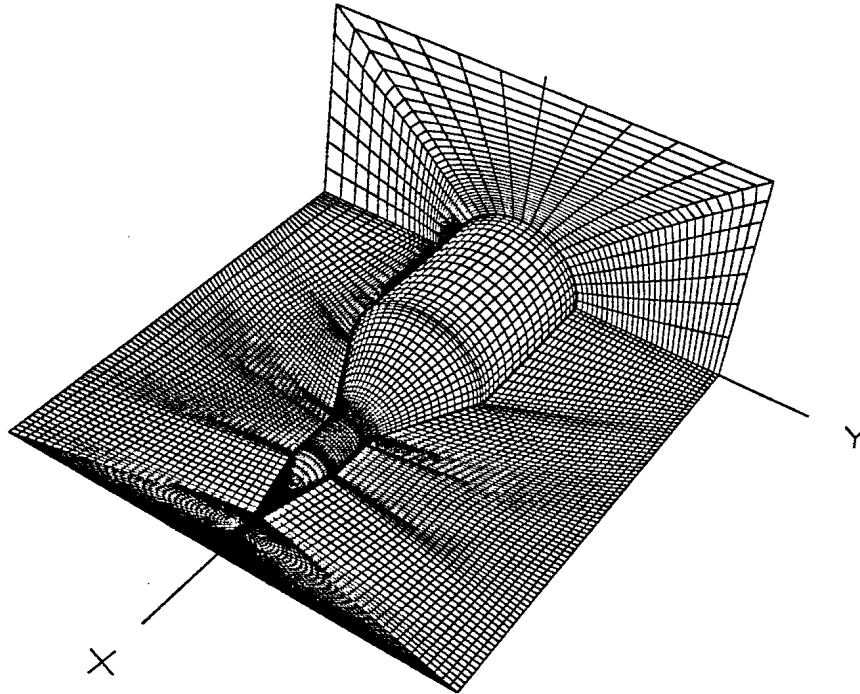


FIGURE 3 - 3D computational domain

The applied boundary conditions for the cases studied in this analysis included a range of Mach numbers from 2.0 to 8.2, for laminar and turbulent flows. Standard sea

UNCLASSIFIED

5

level pressure and temperature were employed, corresponding to conditions present in the aeroballistic range. Additionally, cases were also studied at conditions corresponding to the DRA wind tunnel trials (laminar flow), at Mach number 8.2. Tables I and II summarize the flow conditions employed during these analyses (Ref. 1).

TABLE IDREV Simulations Flight Parameters

Mach Number	2.0 to 8.2
Pressure (N/m ²)	101325.1
Temperature (K)	293.15
Velocity (m/s)	680 to 2788
Re/(projectile length (m))	52.2×10^6 to 214.1×10^6

TABLE IIDRA Wind Tunnel Parameters (Ref. 1)

Mach Number	8.2
Pressure (N/m ²)	839.7
Temperature (K)	89.3
Velocity (m/s)	1553
Re/(projectile length (m))	8.2×10^6

5.0 RESULTS**5.1 Aerodynamic Coefficients****5.1.1 Drag Coefficients**

The drag coefficient in terms of Mach number is shown in Fig. 4. This figure shows two curves: one generated by TASCflow and the other based on experimental results (Ref. 4). It is obvious from this figure that the value of C_D for this projectile is very

UNCLASSIFIED

6

high. For its part, TASCflow was used to compute values of wave drag over the projectile at several Mach numbers, between Mach 2.0 and 8.2. The values of base drag used to transform these wave drag (head drag + skin friction drag) values into total drag (wave drag + base drag) coefficients (to simplify the comparisons with experimental values) come from semi-empirical results (Ref. 6).

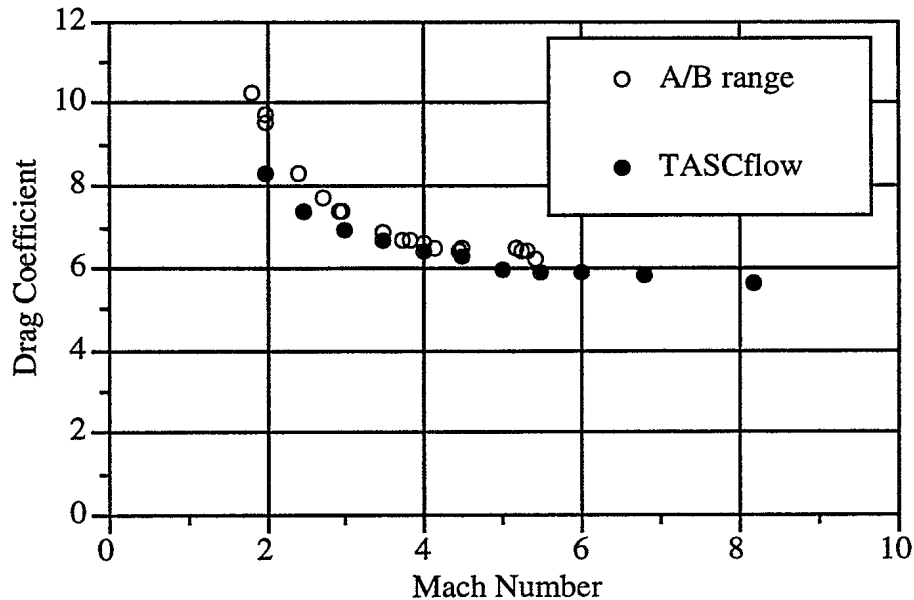


FIGURE 4 - Total drag coefficient of CAN-1 projectile

A comparison between the values obtained with TASCflow and those from the aeroballistic range provides an average relative error of approximately 5%. It should be noted that smaller relative errors exist for the higher Mach numbers (around 3.1% for Mach number 5.5), and conversely, larger relative errors for lower Mach numbers (around 10% at Mach number 2.0). This peculiarity comes from the empirical nature of the CFD base drag values. These empirical drag values were calculated to provide base drag coefficients to adjust the computational results, which only included forebody drag (substantially larger than the base drag for the present Mach number range). It is known that projectile base drag makes up a larger proportion of the total drag as the Mach number decreases. Thus, there is a larger relative error in the empirical term than in the CFD term, and it suggests that the larger relative error in the overall results comes from the empirical calculations.

UNCLASSIFIED

7

The two curves from Fig. 4 present an interesting feature - most notable in the experimental data: they can be divided into two distinct segments, one above and the other below Mach 4.0. Below Mach 4.0, the magnitude of C_D increases rapidly. However, above Mach 4.0, the data shows a relatively small linear variation. For this case (above Mach 4.0), the drag coefficient appears to be declining at a slower rate due to a bow shock/flare interaction. The bow shock interacts with the flare shock leading to increased pressure on the flare. As the Mach number increases the bow shock lies closer to the body surface increasing the effect of this interaction. Figures 5 (a) and 5 (b) show this flow pattern, at Mach 3.5 and 5.5 respectively, for the projectile in free flight. Thus, a general conclusion of this study is that the drag coefficient is highly influenced by the shock wave / flare interaction.

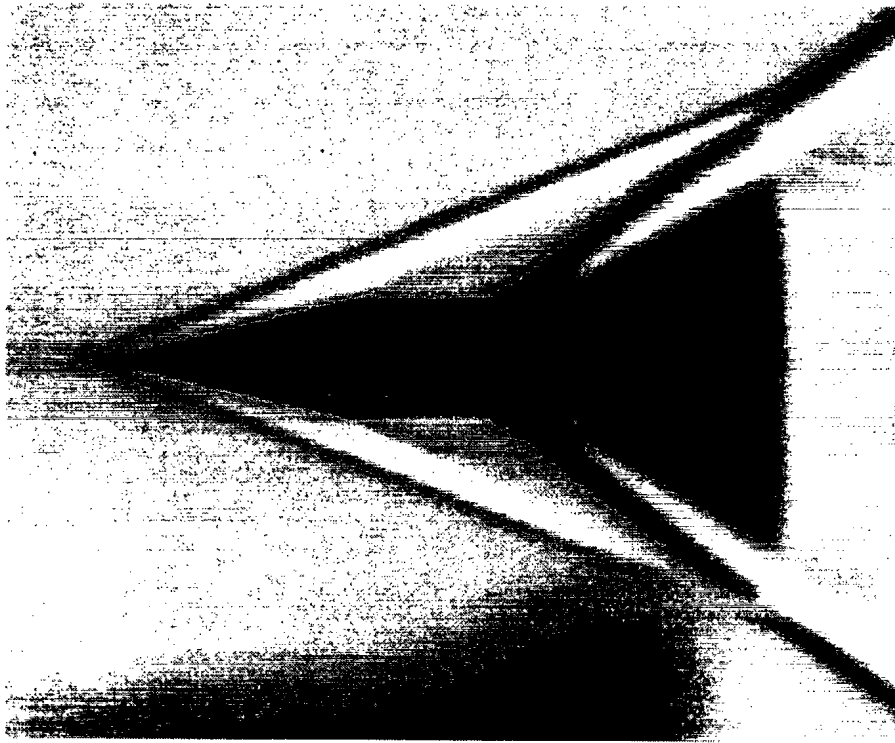


FIGURE 5 (a) - CAN-1 projectile at Mach 3.5

UNCLASSIFIED

8

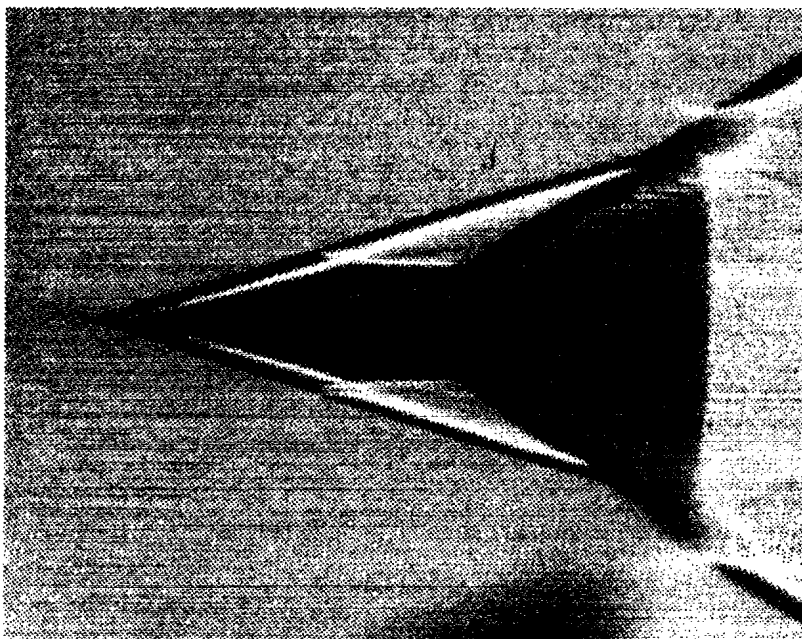


FIGURE 5 (b) - CAN-1 projectile at Mach 5.5

Identical flow features (including shock wave/boundary layer interactions) have also been identified on density maps from CFD cases. Figure 6 presents such a density map at flight conditions similar to the conditions encountered in Fig. 5 (b).

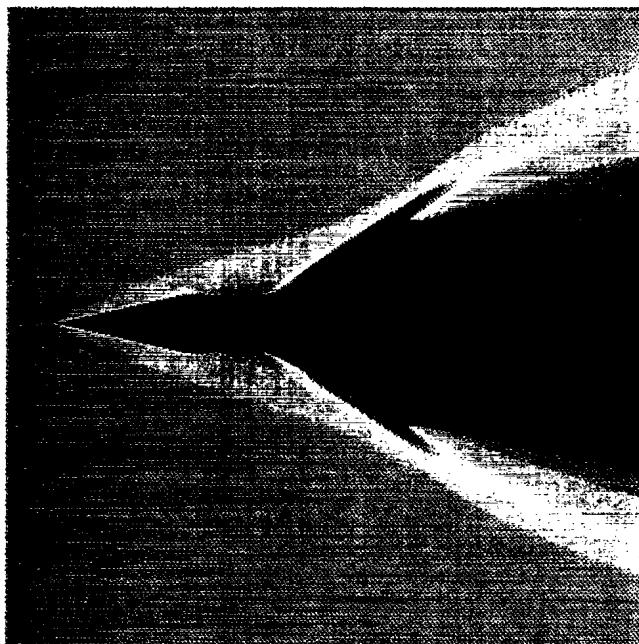


FIGURE 6 - CFD density map at Mach 5.5

UNCLASSIFIED

9

5.1.2 Other Coefficients

As introduced earlier, the grid generated for use with the CFD code was built in such a way to allow for angle of incidence testing of this projectile (grid providing 180° of the projectile). Thus, several aerodynamic coefficients, such as $C_{M\alpha}$ and $C_{N\alpha}$, have also been calculated through CFD computations. Selected cases of these results (corresponding to experimental data) are presented in the following table.

Table III gives the results for the pitch moment coefficient slope ($C_{M\alpha}$) and the normal force coefficient slope ($C_{N\alpha}$), generated through modelling at small angles of attack, and compares them to experimental results from the aeroballistic range. The CFD values ($C_{M\alpha}$ and $C_{N\alpha}$) were calculated by running cases at a fixed angle of incidence (1°), and dividing the computed values of C_N and C_M by this angle.

TABLE III - $C_{M\alpha}$ and $C_{N\alpha}$ comparisons for CAN-1 ($M = 4.5$)

	Experimental	CFD	% relative error
$C_{M\alpha}$	-40.423	-41.092	1.7%
$C_{N\alpha}$	21.689	21.302	1.8%

The values in Table III are for an experimental and a CFD Mach number of 4.50. The experimental value for $C_{M\alpha}$ was calculated from a multiple likelihood method fit through the results of three individual firings. It carries a probable error of $\pm 2.0\%$. With a relative error between the experimental and computational values less than 2.0%, the CFD calculations succeeded in modelling this characteristic of the flow in a satisfactory manner.

The experimental value of $C_{N\alpha}$ was calculated from the results of a single aeroballistic range test, as it was not possible to collect additional information on this variable due to the low angles of attack experienced by the projectiles in flight. Therefore, the error in this value has not been established. However, it should be noticed that a relative error between the numerical and the experimental values of less than 2.0% exists, which implies with a high probability that the CFD calculations succeeded in modelling this characteristic of the flow in a satisfactory manner also.

UNCLASSIFIED

10

5.2 Surface Pressure Survey

Surface pressure information is also obtainable from a CFD analysis, but not from free-flight experimental testing. Figure 7 shows surface pressure plots generated from the TASCflow results for Mach number 4.0, 5.5, 6.8, and 8.2 (the dimensional values of pressure and length are used to allow comparisons with the results from DRA). All 4 curves present very specific information about the flow over this body: initial pressure rise on the flare, effects of the bow shock interaction on the pressure values, and increasing pressure value on the nose and the flare as the Mach number increases. Also, note the large magnitude reached by the pressure at the point of bow shock interaction (on the flare). Additionally, it can be noted that the curve at Mach number 4.0 does not show signs of bow shock interaction, which supports the information introduced earlier on shock/flare interaction. Finally, it can be observed that the shock wave/boundary layer interaction (identified by the peak pressure on the flare) moves upstream along the flare as the Mach number increases, as the shock angle decreases and moves closer to the body.

Figure 8 shows comparative surface pressure curves calculated by the DRA research group (Ref. 1). Comparing the curves from Figs. 7 and 8, it can first be concluded that the pressure surveys for corresponding Mach numbers are very similar. Then, comparing the dimensional values of pressure also shows a very good agreement between the two sets of curves, even if different codes and turbulence models (similar flow conditions) have been employed by the two groups to performed their computations.

UNCLASSIFIED

11

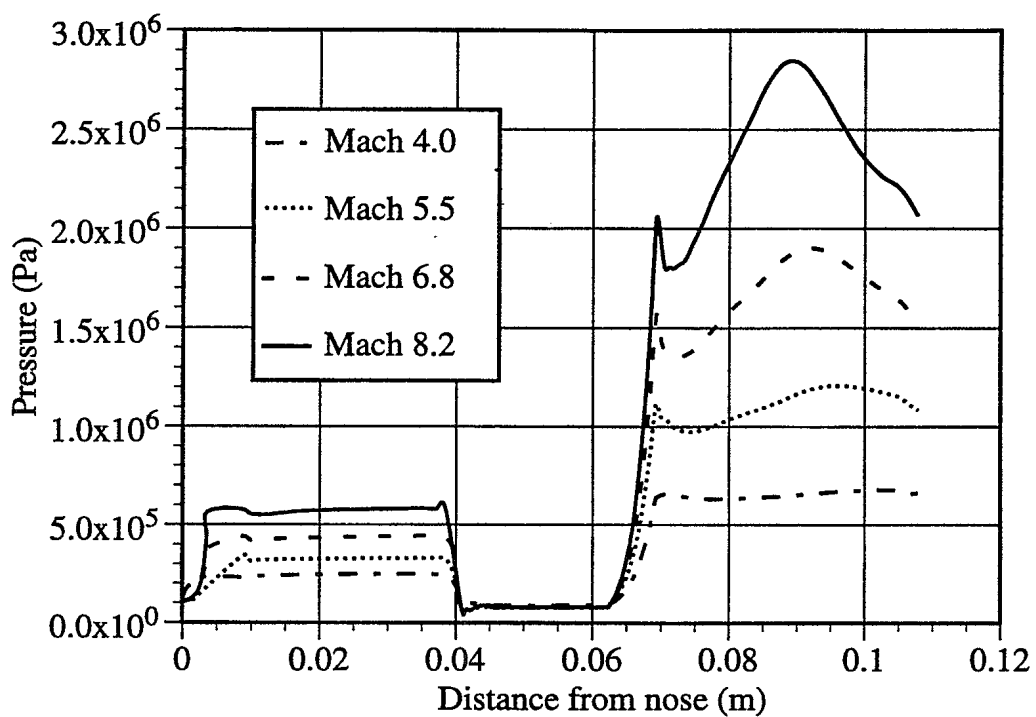


FIGURE 7 - Surface pressure on the CAN-1 projectile

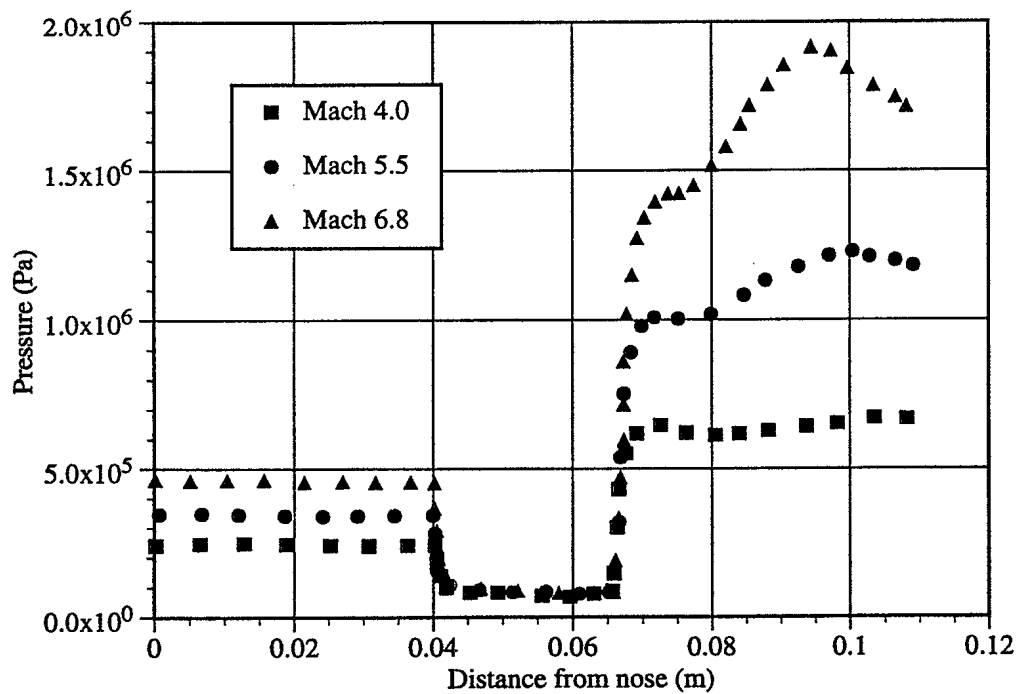


FIGURE 8 - Surface pressure on the CAN-1 projectile (DRA results)

UNCLASSIFIED

12

Figure 9 shows the effects of an angle of incidence of 1.0° on the flare surface pressure at a Mach number of 8.2. Three curves are shown on this figure: a curve at 0° angle of incidence (same curve as previously shown in Fig. 7), and the leeward and the windward curves for the case at 1.0° angle of incidence. The first consequence of this small change in incidence is a difference in the shock wave - flare interaction position between the curve at 0° angle of incidence and the windward and leeward ones. Additionally, the 0° angle of incidence curve has a somewhat larger amplitude than the two other curves. Also, these three curves display the same general shape until the area of the flare corner, where differences begin appearing between the results. Finally, the surface pressure for the leeward side shows a substantial reduction compared to the case at 0° , which could lead to a change in the forces affecting this projectile.

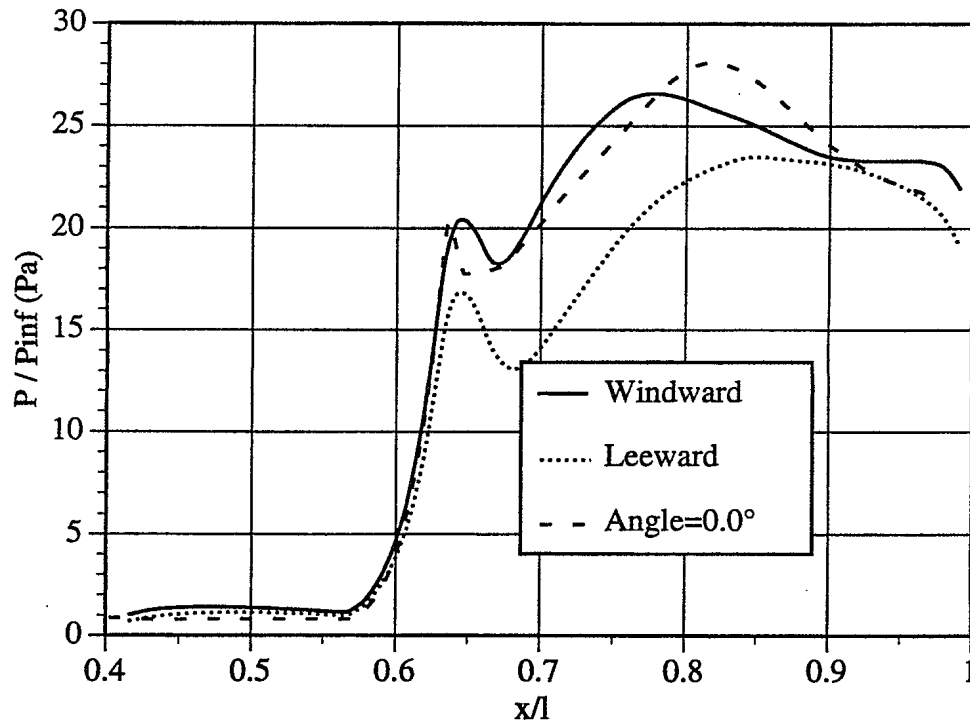


FIGURE 9 - Effects of the angle of incidence on the flare surface pressure

As a final analysis, a study into the possible presence of a separation zone upstream of the flare corner of this projectile was conducted using TASCflow, at conditions corresponding to a DRA wind tunnel experiment. These conditions, presented in Table II, provide Reynolds numbers based on the length of the projectile of 9.0×10^5 , and based on

UNCLASSIFIED

13

the undisturbed boundary layer thickness (thickness between 3.5 and 4.0 mm) of 0.3×10^5 . The flow separation phenomenon was investigated due to its important consequences on the heat transfer process at the surface of the projectile. Reference 9 and Fig. 10 show that the reattachment point at the surface of the flare would be the location with the maximum heat transfer rate, and could therefore present problems with ablation at hypersonic speeds.

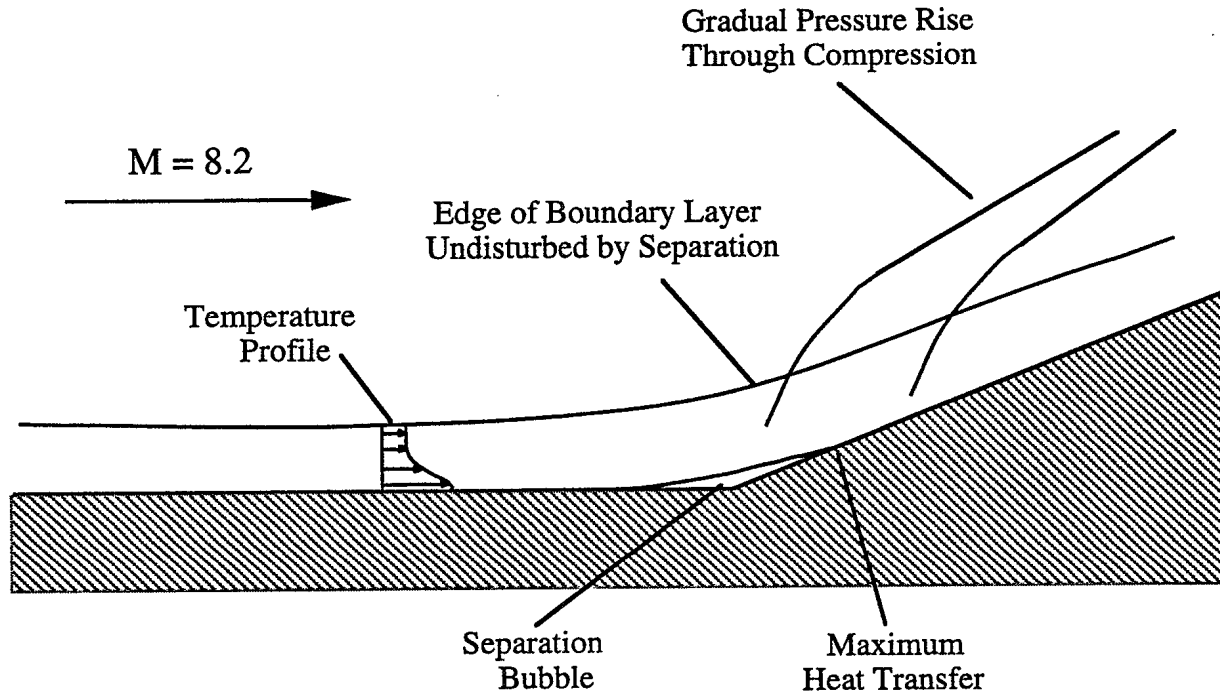


FIGURE 10 - Flowfield for turbulent compression corner with separation

An experimental investigation by Coleman and Stollery (Ref. 10) into incipient separation correlated the onset of separation with respect to Mach number and Reynolds number based on the undisturbed boundary layer thickness. Following the information provided through their analysis, it was concluded that the case under investigation should produce separation, due to the large angle of the flare, and to the specific values of the Reynolds number used (based on the undisturbed boundary layer thickness).

TASCflow was therefore employed to calculate the corresponding flowfield in an attempt to reproduce the experimental results from DRA, which had previously shown some signs of separation (Ref. 7). The coefficient of friction was used to determine the

UNCLASSIFIED

14

position of separation and of reattachment. Figure 11 shows a graph of the coefficient of friction at the surface of the projectile.

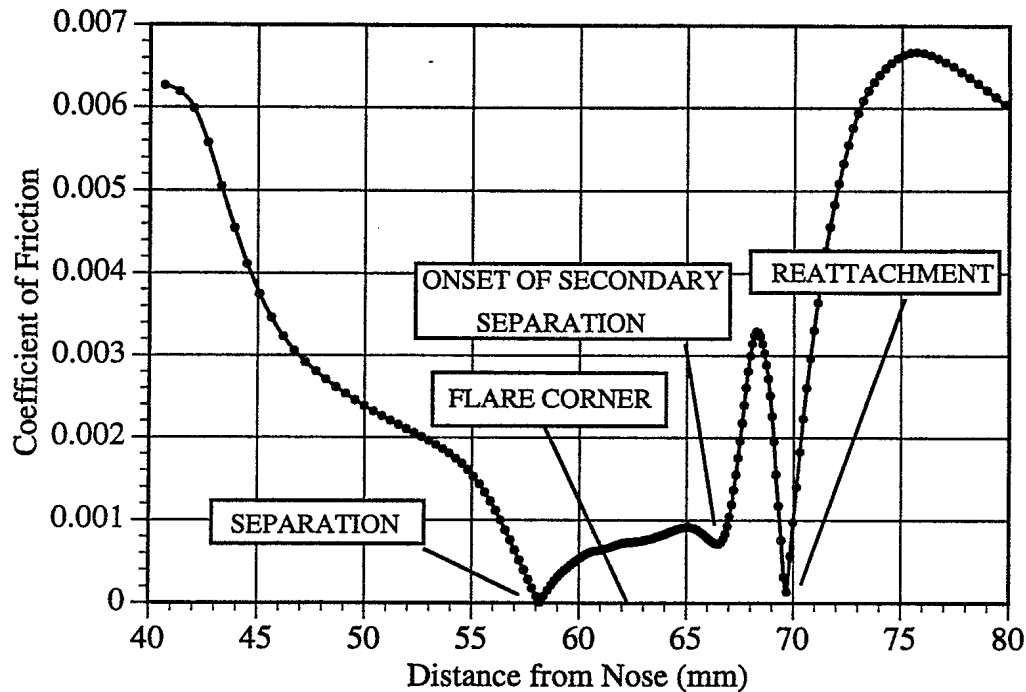


FIGURE 11 - Coefficient of friction for a laminar Mach 8.2 case

Using the coefficient of friction, it is relatively easy to determine the size and location of the separation region on this projectile. With the TASCflow simulation, the separation bubble was calculated to be 11.2 mm long, to begin at around 4.2 mm upstream of the corner of the flare (at around 58.2 mm from the nose), and to reattach at approximately 7 mm downstream from the flare corner (at around 69.4 mm from the nose). Also visible on this figure is the position (between 66 and 67 mm from the nose) of the onset of a secondary separation bubble.

Figure 12 shows the boundary layer profile normal to the cylinder, at a position of 63.8 mm from the nose of the projectile. The loss of momentum of the flow close to the wall, caused by the adverse pressure gradient generated by the flare, causes flow retardation and velocity reversal. The reversed flow velocity reached values corresponding to 35% of the freestream value. Figure 13 shows a speed contour plot of the flare corner area. From the scale at the right of the plot, it is obvious that the velocity in that region is

UNCLASSIFIED

15

oriented in a direction opposite to the freestream flow. Thus, TASCflow was able to simulate the physical characteristics of this separated flow, and confirm that a separation region exists upstream of the flare.

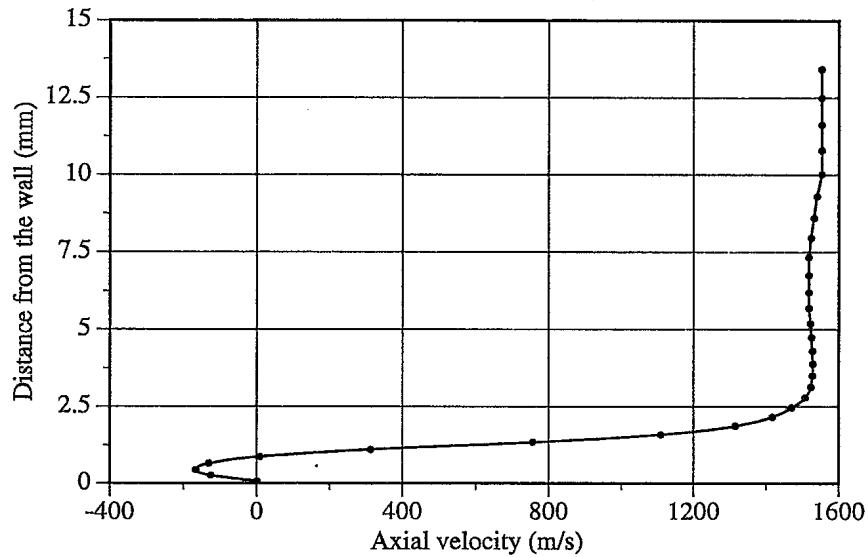


FIGURE 12 - Boundary layer profile at 63.8 mm from the nose

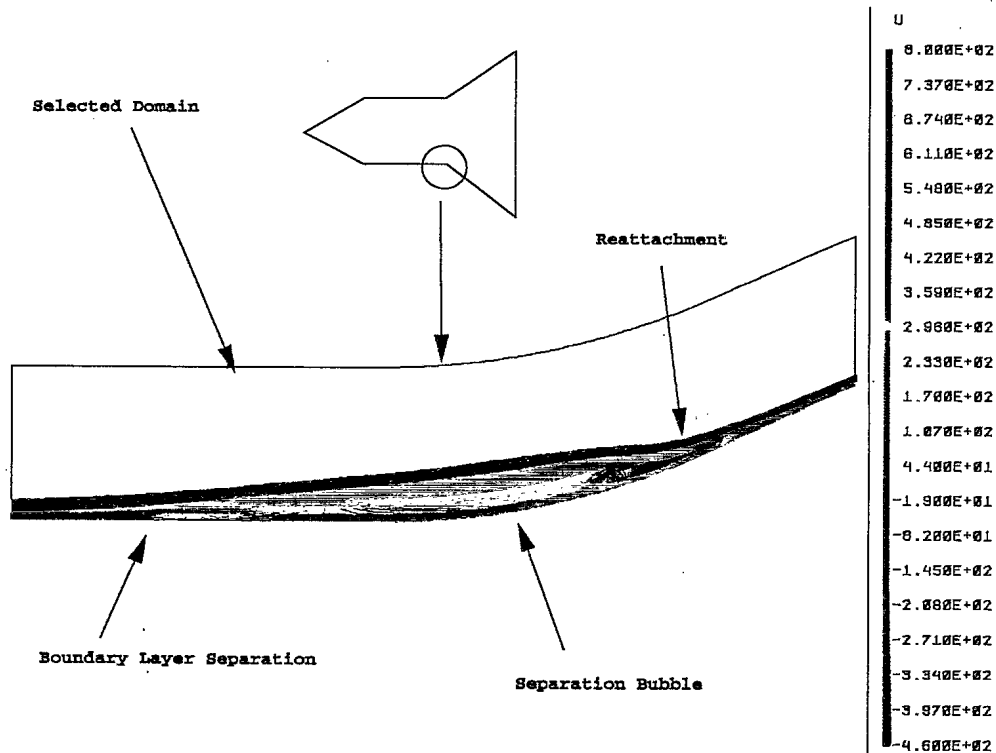


FIGURE 13 - Separation zone at flare corner (CFD)

UNCLASSIFIED

16

6.0 CONCLUSIONS

The phase of the overall research programme presented in this memorandum covered only the numerical analysis of the aerodynamic characteristics of one of the configurations designed for experimental testing. Pressure surveys, aerodynamic coefficient calculations and visualization of the flow around the projectile were accomplished for a range of Mach numbers and angles of incidence.

The conclusions derived from this investigation can be divided into two distinct sections: the ones related to the projectile and to the aerodynamic characteristics surrounding it, and the others about the methods employed to perform this analysis.

On the flow side, a recirculation region has been identified at the compression corner for a low Reynolds number laminar case (corresponding to British wind tunnel conditions). Through CFD analysis, several variables related to this phenomenon have been identified and quantified.

Through computational fluid dynamic calculations (CFD), it was also possible to model the flow characteristics around an hypersonic projectile with an acceptable accuracy. Validation of these results against free-flight data allowed the extension of the useful range of this code to include low hypersonic Mach numbers. However, as presented in the introduction, real gas effects were not considered in the calculations (calculations in the low hypersonic speed range, thus only small errors were involved in neglecting real gas effects). The drag coefficient of the CAN-1 projectile has been determined to be very high, and to present a nonlinear variation over the tested Mach number range. Additionally, the values of $C_{M\alpha}$ and $C_{N\alpha}$ also agreed well with experimental data. Other types of results, including pressure surveys and the location of separation, were not available through aeroballistic range testing. Nevertheless, the results produced by CFD were compared to data available in the literature, and from DRA, with good agreement. However, the lack of computer facilities allowing us to develop a grid including the base flow region led to problems in analyzing the results, and added an extra source of errors in the results (empirical values).

UNCLASSIFIED

17

7.0 RECOMMENDATIONS

Following the present investigation, it is recommended:

- to perform additional CFD, and possibly Laser Doppler Velocimetry measurements at the compression corner to identify specific variables of the separation region in turbulent conditions. Study the underlining principles under this separation phenomena and the variables affecting it;
- to perform additional CFD investigations on hypersonic models incorporating calculations of the base region.

8.0 ACKNOWLEDGEMENTS

We would like to acknowledge the assistance of Dr. J. Edwards of DRA for his assistance through the duration of this study.

UNCLASSIFIED

18

9.0 REFERENCES

- 1 - Dupuis, A.D. and Edwards, J.A., "Free-Flight Tests, Analysis and Aeroheating Aspects of Two Hypersonic Configuration," AIAA Paper No. 95-0333, AIAA 33rd Aerospace Sciences Meeting and Exhibit, Reno, Nevada, January 9-12, 1995.
- 2 - Dupuis, A.D. and Drouin, G., "The DREV Aeroballistic Range and Data Analysis System," AIAA Paper No. 88-2017, AIAA 15th Aerodynamic Testing Conference, San Diego, California, May 18-20, 1988.
- 3 - "Ballistic Range Data Analysis System (BARDAS)," Arrow Tech Associates Inc., DREV Contract No. W7701-0-1227, March 1992.
- 4 - Dupuis, A. D., Edwards, J. A. and Normand, M., "Aerodynamic Characteristics and Aeroheating Aspects of Two Hypersonic Configurations from Free-Flight Tests," DREV TR-9428, October 1995, UNCLASSIFIED.
- 5 - "TASCflow - Version 2.3 : Theory and User Documentation," ASC Advanced Scientific Computing Limited, Waterloo, Ontario, Canada (01/1994).
- 6 - Mueller, T.J., "Determination of the Turbulent Base Pressure in Supersonic Axisymmetric Flow," AIAA Paper No. 67-446, AIAA 3rd Joint Propulsion Specialist Conference, Washington, Washington D.C., July 17-21, 1967.
- 7 - Edwards, J. A. and Dupuis, A. D., "Computational Analysis of the CAN-1 Hypersonic Research Projectile," 19th TTCP WTP-2 Meeting, Bedford, UK, June 1994.
- 8 - Roper, J. J., "A Computational Investigation of Unsteady Shock-Boundary Layer Interaction," DRA Report # DRA/DWS/WX7/TR95819, September 1995, UNCLASSIFIED.

UNCLASSIFIED

19

- 9 - Babinsky, H. and Edwards, J. A., "On the Incipient Separation of a Turbulent Hypersonic Boundary Layer," DRA Fort Halstead, to be published.
- 10 - Coleman, G.T. and Stollery, J.L., "Incipient Separation of Axially Symmetric Hypersonic Turbulent Boundary Layers," AIAA Journal, Vol. 12, No. 1, January 1974, pp. 119-200.

UNCLASSIFIED

INTERNAL DISTRIBUTION

DREV - TM - 9607

1 - Deputy Director General
1 - Head Delivery Systems Section
6 - Document Library
1 - E. Y. Fournier (author)
1 - A. D. Dupuis (author)
1 - G. Dumas
1 - F. Lesage
1 - B. Girard
1 - A. Jeffrey
1 - G. Drouin
1 - R. Delagrave
1 - G. Bérubé
1 - P. Twardawa

UNCLASSIFIED

EXTERNAL DISTRIBUTION
DREV - TM - 9607

2 - DSIS

1 - CRAD

1 - DSAL

1 - DLR

1 - DAR (FT)

1 - DSAA

1 - DSAM

1 - DAEPM(FT)

1 - DRES

4 - Dr. J. Edwards

(2 for further UK distribution)

1 - Dr. Ian Stone

1 - Mr. C. Hilderbrands

1 - Mr J. J. Roper

DRA Military Division

Fort Halstead

Sevenoaks

Kent TN14 7BP

England

1 - Dr. C. Berner

Institut franco-allemand de recherches

5, rue du Général Cassagnou

B. P. 34

68301 - Saint-Louis (France)

1 - Dr. B. J. Walker

AMSMI-RD-SS-AT

Commander

U. S. Army Missile Command

Redstone Arsenal, AL

35898-5252

UNCLASSIFIED

1 - Dr. P. Plostins

SLCBR-LF-F

Army Research laboratory

Aberdeen Proving Ground

Maryland 21005-5066

USA

1 - Mr. A. J. Sadler

Head AP6

Weapons Aerodynamics Division

DRA

Bedford MK41 6AE

England

1 - Dr. J. Gardner

DSTO

Surveillance Research Laboratory

P.O. Box 1500

Salisbury, SA 5108

Australia

1 - Dr. K. Krishnamoorthy

DSTO

Weapons Systems Division

P.O. Box 1500

Salisbury, SA 5108

Australia

1 - Dr. P. Sullivan

University of Toronto

Institute for Aerospace Studies (UTIAS)

4925 Dufferin St

Downsview, ON

M3H 5T6

UNCLASSIFIED
 SECURITY CLASSIFICATION OF FORM
 (Highest classification of Title, Abstract, Keywords)

DOCUMENT CONTROL DATA		
1. ORIGINATOR (name and address) DREV	2. SECURITY CLASSIFICATION (Including special warning terms if applicable) UNCLASSIFIED	
3. TITLE (its classification should be indicated by the appropriate abbreviation (S,C,R or U)) COMPUTATIONAL FLUID DYNAMIC ANALYSIS OF THE CAN-1 HYPERSONIC RESEARCH PROJECTILE		
4. AUTHORS (Last name, first name, middle initial. If military, show rank, e.g. Doe, Maj. John E.) FOURNIER, E.Y., DUPUIS, A.D.		
5. DATE OF PUBLICATION (month and year) JUNE 1996	6a. NO. OF PAGES 24	6b. NO. OF REFERENCES 10
7. DESCRIPTIVE NOTES (the category of the document, e.g. technical report, technical note or memorandum. Give the inclusive dates when a specific reporting period is covered.) DREV Technical Report		
8. SPONSORING ACTIVITY (name and address) Delivery Systems Section		
9a. PROJECT OR GRANT NO. (Please specify whether project or grant) 02EA19	9b. CONTRACT NO. .	
10a. ORIGINATOR'S DOCUMENT NUMBER <i>TM-9607</i>	10b. OTHER DOCUMENT NOS. N/A	
11. DOCUMENT AVAILABILITY (any limitations on further dissemination of the document, other than those imposed by security classification) <input checked="" type="checkbox"/> Unlimited distribution <input type="checkbox"/> Contractors in approved countries (specify) <input type="checkbox"/> Canadian contractors (with need-to-know) <input type="checkbox"/> Government (with need-to-know) <input type="checkbox"/> Defence departments <input type="checkbox"/> Other (please specify) :		
12. DOCUMENT ANNOUNCEMENT (any limitation to the bibliographic announcement of this document. This will normally correspond to the Document Availability (11). However, where further distribution (beyond the audience specified in 11) is possible, a wider announcement audience may be selected.)		

UNCLASSIFIED
 SECURITY CLASSIFICATION OF FORM

UNCLASSIFIED
SECURITY CLASSIFICATION OF FORM

13. **ABSTRACT** (a brief and factual summary of the document. It may also appear elsewhere in the body of the document itself. It is highly desirable that the abstract of classified documents be unclassified. Each paragraph of the abstract shall begin with an indication of the security classification of the information in the paragraph (unless the document itself is unclassified) represented as (S), (C), (R), or (U). It is not necessary to include here abstracts in both official languages unless the text is bilingual).

In an effort to broaden our knowledge base on hypersonic aerodynamics, DREV conducted a Computational Fluid Dynamics (CFD) analysis on a hypersonic projectile, and successfully validated the analysis with results from free flight trials. Quantitative information (aerodynamic coefficients, shock wave interaction position, separation bubble position, etc.) was accurately obtained by the CFD code, as indicated by the good agreement with experimental results. The influence of the shock wave/flame interaction on some of these quantities was also identified. On the qualitative side, the modelling of flow characteristics such as shock patterns and positions, flow separation effects, etc, in a hypersonic environment has been accomplished. In addition, comparisons between these results and those from a numerical analysis from the Defence Research agency (DRA) have shown that they provide similar values.

14. **KEYWORDS, DESCRIPTORS or IDENTIFIERS** (technically meaningful terms or short phrases that characterize a document and could be helpful in cataloguing the document. They should be selected so that no security classification is required. Identifiers, such as equipment model designation, trade name, military project code name, geographic location may also be included. If possible keywords should be selected from a published thesaurus. e.g. Thesaurus of Engineering and Scientific Terms (TEST) and that thesaurus-identified. If it is not possible to select indexing terms which are Unclassified, the classification of each should be indicated as with the title.)

AERODYNAMIC COEFFICIENTS
HYPERSONIC
CFD
SEPARATION

UNCLASSIFIED
SECURITY CLASSIFICATION OF FORM

Requests for documents
should be sent to:

DIRECTOR SCIENTIFIC INFORMATION SERVICES

Dept. of National Defence

Ottawa, Ontario

K1A 0K2

Tel: (613) 995-2971

Fax: (613) 996-0392

NO. OF COPIES NOMBRE DE COPIES	COPY NO. COPIE N°	INFORMATION SCIENTIST'S INITIALS INITIALES DE L'AGENT D'INFORMATION SCIENTIFIQUE
AQUISITION ROUTE FOURNI PAR ► DREV		
DATE ► 21 Aug 96		
DSIS ACCESSION NO. NUMÉRO DSIS ►		

DND 1158 (6-87)



National
Defence

Défense
nationale

499218

**PLEASE RETURN THIS DOCUMENT
TO THE FOLLOWING ADDRESS:**

DIRECTOR
SCIENTIFIC INFORMATION SERVICES
NATIONAL DEFENCE
HEADQUARTERS
OTTAWA, ONT. - CANADA K1A 0K2

**PRIÈRE DE RETOURNER CE DOCUMENT
À L'ADRESSE SUIVANTE:**

DIRECTEUR
SERVICES D'INFORMATION SCIENTIFIQUES
QUARTIER GÉNÉRAL
DE LA DÉFENSE NATIONALE
OTTAWA, ONT. - CANADA K1A 0K2

Toute demande de document
doit être adressée à:

DIRECTEUR - SERVICES D'INFORMATION SCIENTIFIQUE

Ministère de la Défense nationale

Ottawa, Ontario

K1A 0K2

Téléphone: (613) 995-2971

Télécopieur: (613) 996-0392